Dephasing effect of Rydberg states on trap loss spectroscopy of cold atoms

YIFEI CAO,[1,2] WENGUANG YANG,[1,2] HAO ZHANG,[1,2] MINGYONG JING,[1,2] WEIBIN LI,[3] LINJIE ZHANG,[1,2,*] LIANTUAN XIAO,[1,2] AND SUOTANG JIA[1,2]

[1]*State Key Laboratory of Quantum Optics and Quantum Optics Devices, Institute of Laser Spectroscopy, Shanxi University, Taiyuan, Shanxi 030006, China*
[2]*Collaborative Innovation Center of Extreme Optics, Shanxi University, Taiyuan, Shanxi 030006, China*
[3]*School of Physics and Astronomy, and Centre for the Mathematics and Theoretical Physics of Quantum Non-equilibrium Systems, University of Nottingham, Nottingham, NG7 2RD, United Kingdom*
[*]*zlj@sxu.edu.cn*

Abstract: In this paper, we investigate the asymmetry of trap loss spectra of ultra cold atoms during the excitation of Rydberg states. It is shown that the profile of trap loss spectrum is affected by the density of Rydberg atoms as well as dephasing rate of Rydberg states. The splitting of trap loss spectrum is shown at the higher dephasing rates of Rydberg states. A three-level model, where the dephasing rates mainly ascribe to a random collision of Rydberg atoms, reasonably explains the experimental results.

1. Introduction

Rydberg atoms possess large dipole moments and long lifetimes, which are important for generating collectivity and entanglement for quantum computation and quantum simulation [1–5]. At present, Rydberg atoms with high principal quantum numbers are suitable for quantum measurement due to sensitive response to external electric fields [6–10]. In quantum computation, quantum simulation and precision measurement, the dephasing rate directly affects the coherence time of the quantum states [11–13]. Typically detecting techniques currently of cold Rydberg atoms includes: selective field ionization and electromagnetically induced transparency spectroscopy. Selective field ionization, which ions or electrons from ionized Rydberg atoms were detected, has been widely used in transition dipole moment measurement [14, 15], quantum defect measurement [16], lifetime measurement [17], collision cross section measurement of Rydberg states [18, 19], etc. As a non-destructive detection technique, electromagnetic induced transparent spectroscopy is used in the study of Rydberg atom interaction [20], Rydberg atom interaction with the field [21, 22] and Rydberg excitation light frequency stabilization [23]. Similarly, trap loss spectroscopy is also a non-destructive measurement technology and has been widely used in the field of ultra cold atoms, especially in ultra cold molecular spectroscopy, which has achieved the measurement of the vibrational state and molecular vibrational coefficient of Cs_2 molecule [24].

In this work, the effect of dephasing rate of Rydberg states on trap loss spectra of the ultra cold Rydberg atoms is studied. The two-photon excitation of Rydberg states is employed in a standard magneto-optical trap(MOT). The trap loss of MOT occurred as the production of Rydberg atoms. By varying the detuning of cooling laser, the trap loss spectra are obtained at different densities, and the shape of the trap loss spectra was simulated using a ladder-type three-level system. We employ a theoretical model of atoms collision and the master equation calculation to explain well our experimental data.

2. Experimental setup

The experimental setup is shown in Fig.1(a), where an ultra cold atom gases with an atom number of around 9×10^6 and a temperature of about 200 μK is obtained using laser cooling techniques. Its peak density can be tuned in the range of 0.6×10^{10} cm^{-3} to 6×10^{10} cm^{-3} by adjusting detuning of cooling laser. The ultra cold atoms maintain the steady states of cyclic transition between the energy levels $6S_{1/2}$ (F=4) and $6P_{3/2}$ (F = 5). Then a laser beam with a wavelength of 510 nm is added into the ultra cold atom gases to couple the transition from the $6P_{3/2}$(F=5) to $51S_{1/2}$ Rydberg state. The energy level diagram is shown in Fig.1(b), where the cooling laser and repumping laser are provided by commercial semiconductor laser(DL-Pro, 852 nm) with a waist about 400 μm. The frequency is locked by saturation absorption spectroscopy on the transition from $6S_{1/2}$(F=4) to $6P_{3/2}$(F=5) and $6S_{1/2}$(F=3) to $6P_{3/2}$(F=4) with about 1 MHz linewidth. The excitation light (wavelength 510 nm) has a waist of about 800 μm at the MOT. In the experiment, the excitation light is optimized to ensure complete coverage of the atoms. The frequency of excitation light is locked to the transition from $6P_{3/2}$ to $51S_{1/2}$ through the super-stable cavity, and its linewidth is less than 100 Hz.

The Rabi frequencies of the excitation laser and cooling laser are $2\pi \times 0.8$ MHz and $2\pi \times 45$ MHz, respectively. During the experiment, we scan the frequency of the Rydberg excitation laser at the resonance position with the frequency range of 75 MHz. The fluorescence is detected by a collection system with the lens area of 50.67 mm^2 and the distance of 11 mm from the atom cloud, giving the trap loss spectra of ultra cold cesium atoms. And a 852 nm narrow-bandwidth optical filter is used to eliminate the effects of stray light. In order to improve the signal-to-noise ratio of the spectral signal, we use a frequency modulation technique [25], which effectively improves the signal-to-noise ratio by about 30 dB.

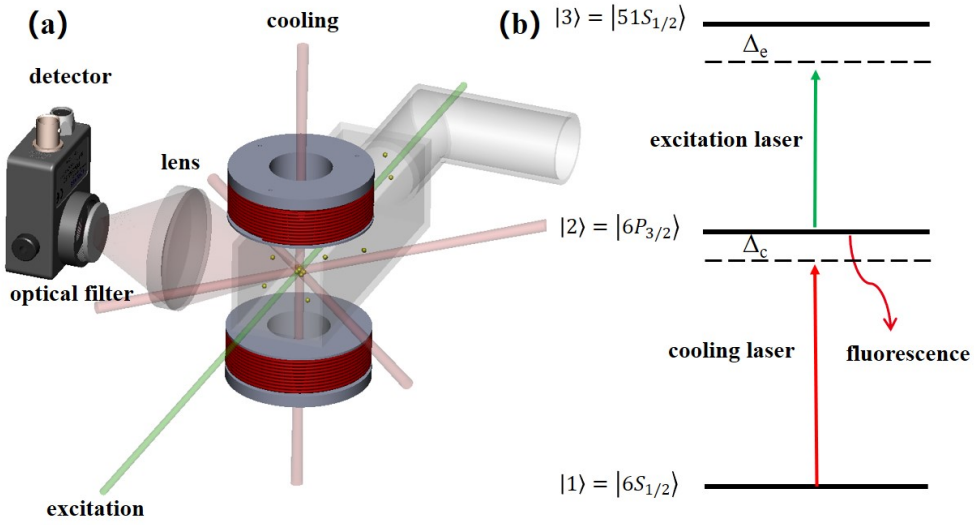

Fig. 1. (a) Sketch of the experimental set up, the 510 nm excitation laser and 852 nm cooling laser are propagated into a cold cesium atom cloud, and the fluorescence collection device detects the fluorescence signal emitting by the atoms; (b) Cesium Rydberg atom ladder-level system schematic.

3. Result and discussion

The results are shown in Fig.2, where the cooling laser Rabi frequency is $2\pi \times 45$ MHz, the Rydberg excitation laser Rabi frequency is $2\pi \times 0.8$ MHz, and the excitation laser frequency is scanned from -75 MHz to 75 MHz near the resonance of $6P_{3/2} \rightarrow 51S_{1/2}$. The density of atoms

are 8.53×10^8 cm^{-3}(Fig.2(a)) and 4.92×10^9 cm^{-3}(Fig.2(b)), respectively. It can be shown that when the density of atoms increases, the trap loss spectra show a clear asymmetric splitting.

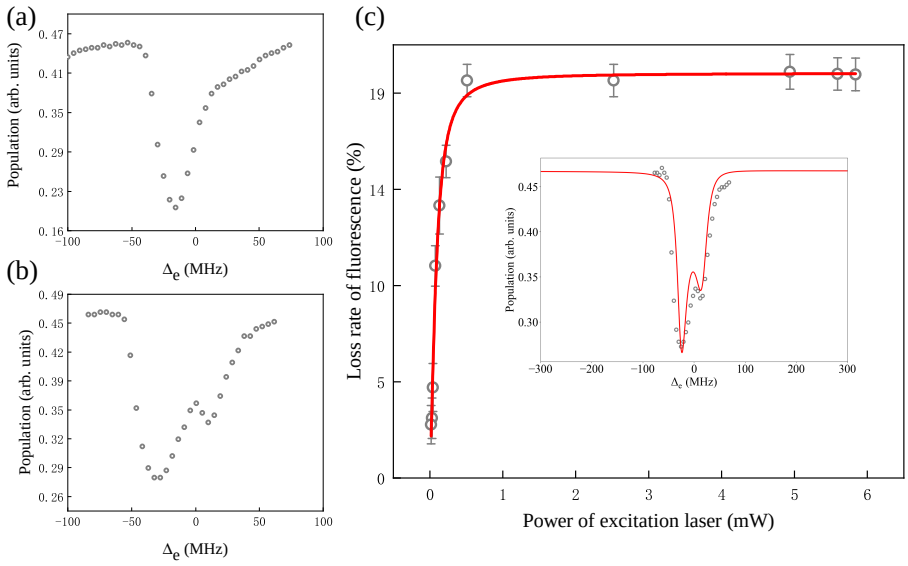

Fig. 2. (a) Trap loss spectrum of atom density 8.53×10^8 cm^{-3}; (b) Trap loss spectrum of atom density 4.92×10^9 cm^{-3}; (c) Rydberg atom saturation excitation curve with atom density 4.92×10^9 cm^{-3}, in which the inset figure shows the result of fitting the maximum fluorescence loss with the theoretical model, where the gray circles are experimental data and the solid red curve is the theoretical calculation result.

To explain the experimental results, we consider a three-level system composed of state $|1\rangle$,$|2\rangle$ and $|3\rangle$(see Fig.1(b)) whose Hamiltonian can be described as:

$$H = H_0 + H_{AL} \tag{1}$$

where H_0 is the Hamiltonian of the system in the absence of external fields and H_{AL} is the Hamiltonian of the light-atom interaction. The strength of the light-atom interaction is described using the Rabi frequency:

$$\Omega = \frac{\mu_{ij}}{\hbar}\sqrt{\frac{2P}{\pi\omega^2 c\varepsilon_0}} \tag{2}$$

where μ_{ij} denotes the dipole leap matrix element of the atom from quantum state $|i\rangle$ to $|j\rangle$, and P and ω are the power and waist of the laser. c and ε_0 are the speed of light and the dielectric constant in vacuum. $\hbar$ is the Planck constant.

The Hamiltonian H can be expressed in the case of considering the rotating wave approximation as:

$$H = \frac{\hbar}{2}\begin{pmatrix} 0 & \Delta_c & 0 \\ \Omega_c & -2\Delta_c & \Omega_e \\ 0 & \Omega_e & -2(\Delta_c + \Delta_e) \end{pmatrix} \tag{3}$$

where Ω_c and Ω_e denote the Rabi frequencies of the cooling and excitation laser, respectively, and Δ_c and Δ_e are the detuning of the the cooling and excitation laser(see Fig.1(b)).

Taking the Hamiltonian into the Lindblad master equation:

$$\dot{\rho} = -\frac{i}{\hbar}[H, \rho] + L(\rho) \tag{4}$$

$\mathrm{L}(\rho)$ is the Lindblad super operator to describe the dissipative process of the system [26]. In the three-energy system, it takes the following form:

$$L(\rho) = \begin{pmatrix} \gamma_2\rho_{22} & -\frac{1}{2}\gamma_2\rho_{12} & -\frac{1}{2}\gamma_3\rho_{13} \\ -\frac{1}{2}\gamma_2\rho_{21} & -\gamma_2\rho_{22} + \gamma_3\rho_{33} & -\frac{1}{2}\left(\gamma_2 + \gamma_3\right)\rho_{23} \\ -\frac{1}{2}\gamma_3\rho_{31} & -\frac{1}{2}\left(\gamma_2 + \gamma_3\right)\rho_{32} & -\gamma_3\rho_{33} \end{pmatrix} \tag{5}$$

where γ_2 and γ_3 denote the dephasing rates of the excited state $|2\rangle$ ($6\mathrm{P}_{3/2}$) and the Rydberg state $|3\rangle$ ($51\mathrm{S}_{1/2}$), respectively. $\gamma_2 = \gamma_{eg} + \gamma_e$, where γ_{eg} is the decoherence rate due to the spontaneous radiation of the excited state, and γ_e is the decoherence rate due to the interaction of the excited state atoms. Since the effect of the interaction of the excited state atoms is much smaller than their spontaneous radiation, we have:$\gamma_2 \approx \gamma_{eg} = 5.2$ MHz. $\gamma_3 = \gamma_{re} + \gamma_r$,where γ_{re} and γ_r are the decay of the Rydberg atoms, because of the spontaneous radiation and interaction between them.

Since continuous laser excitation is used in the experiment, we use the steady-state solution of the master equation to obtain the change in the distribution of the excited state atom number, i.e., the change of the fluorescence intensity. At the steady state of the system we have: $\dot{\rho}_{ij} = 0$ and $\rho_{11} + \rho_{22} + \rho_{33} = 1$, it means that the total distribution probability of the three quantum states is 1. The excited state atom number distribution can be obtained by solving ρ_{22}:

$$\rho_{22} = \frac{4\left(\Delta_e + \Delta_c\right)^2\Omega_e^2}{4\gamma_2^2\left(\Delta_e + \Delta_c\right)^2 + \left(-4\Delta_c\left(\Delta_c + \Delta_e\right) + \Omega_e^2\right)^2 + 2\left(4\left(\Delta_e + \Delta_c\right)^2 + \Omega_e^2\right)\Omega_c^2 + \Omega_c^4} \tag{6}$$

In the experiment, we first determine the saturation excitation power of Rydberg atoms to ensure that the atoms achieve saturation excitation at the minimum excitation laser power(see Fig.2(c)). It means that the density of Rydberg atoms is only related to the density of ground state atoms. And the effect of van der Waals interaction between atoms can be ignored by using the minimum saturation excitation power [27, 28]. We change the ground state atoms density by controlling the detuning of the cooling laser. Using the expression (6), we have fitted the experimental data theoretically to obtain the dephasing rates γ_3 of the Rydberg states at different atom densities through the fluorescence loss rate. It is shown in the inset figure in Fig.2(c), where the circle is experimental data and the solid curve is the theoretical calculation.

The Fig.3(a) shows the fluorescence loss rate changed with the dephasing rate γ_3. It is obvious from the experimental results that the dephasing rate of the Rydberg states varies linearly with the density of atom clouds. For this phenomenon, we use the random collision model to explain it [18]. Compared to the ground state atoms, the Rydberg atoms have larger atomic radii, so the effect of the ground state atoms collisions can be neglected at the lower atom density [29], and only the collisions between Rydberg atoms are considered. The dephasing rate of the Rydberg state: $\gamma_3 = \gamma_{re} + \gamma_r$, where γ_r is the dephasing rate caused by atom collisions. According to the random collision model:

$$\gamma_r = \sigma_r v_r \rho_r \tag{7}$$

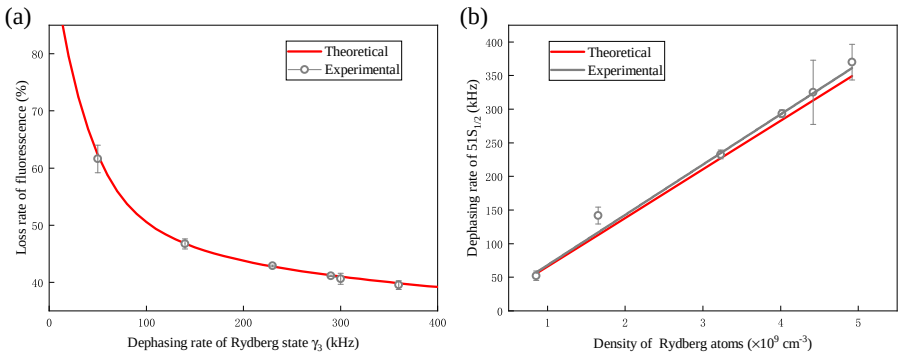

Fig. 3. (a) The fluorescence loss rate varies with the dephasing rate γ_3 of Rydberg state, where the red curve is the theoretical calculation result and the gray circle is the fluorescence loss rate measured experimentally; (b) The dephasing rate γ_3 of Rydberg state varies with the density of Rydberg atoms, where the red curve is the theoretical calculation result and the gray curve is the fitting result of experimental data.

where v_r is the velocity of the Rydberg atom, calculated using the temperature of the cold atoms, which has an average velocity of 17 cm/s for a cold atoms at 200 μK. ρ_r is the density of Rydberg atoms, obtained by scaling the distribution of quantum states in the theoretical model, using the density of excited atoms of state. σ_r is the collision cross section of the Rydberg atom. According to the experimental conditions, the blocking radius of the Rydberg atom is about 22.11 μm, and its collision cross section $\sigma_r = 3.80 \times 10^{-6}$ cm^2.

For the experimental results, we have fitted the result by using a linear function: $y = ax + b$, as shown in Fig.3(b). Where the solid gray line is the result of the linear fit, where $a = 7.74 \times 10^{-8}$ kHz·cm^{-3} and $b = 3.64$ kHz. The red solid line is the result obtained by our model $\gamma_3 = \gamma_{re} + \sigma_r v_r \rho_r$, calculated with a slope of $\sigma_r v_r = 6.46 \times 10^{-8}$ kHz·cm^{-3}. The theoretical model is in good agreement with the experimental results, and the slope of the experimental results obtained is slightly higher than the theoretical calculation, probably due to the fact that the cold atom is heated by the excitation process of the Rydberg atoms during the experiment. The slope of the obtained experimental results is slightly higher than the theoretical calculation because the atomic average velocity used in the theoretical calculation is difference from Gaussian distribution for actual atom gases. In addition, the collision of ground atoms and Rydberg atoms can also lead to higher dephasing rate [29].

4. Conclusion

We have studied the trap loss spectra of the Rydberg atom of the ladder type three-level system in an ultra cold cesium atom and obtained the Rydberg energy level dephasing rate γ_3 and the dependence on atom density. This phenomenon is mainly caused by increase the collision probability of Rydberg atoms by the increasing density, which in turn leads to the decoherence effect. The results of this paper provide a detailed investigation for the dephasing rate of the Rydberg energy levels.

Funding.
This work is supported by the Natural Science Foundation of China, (Nos.61827824, 61475090) and National Key Research and Development Program (No.2017YFA0304203).

Disclosures. The authors declare no conflicts of interest.

References

1. D. Jaksch, J. I. Cirac, P. Zoller, S. L. Rolston, R. Côté, and M. D. Lukin, "Fast quantum gates for neutral atoms," Phys. Rev. Lett. **85**, 2208 (2000).
2. M. D. Lukin, M. Fleischhauer, R. Côté, L. Duan, D. Jaksch, J. I. Cirac, and P. Zoller, "Dipole blockade and quantum information processing in mesoscopic atomic ensembles," Phys. Rev. Lett. **87**, 037901 (2001).
3. H. Weimer, M. Müller, I. Lesanovsky, P. Zoller, and H. P. Büchler, "A rydberg quantum simulator," Nat. Phys. **6**, 382–388 (2010).
4. T. Pohl, C. Adams, and H. Sadephpour, "Cold rydberg gases and ultra-cold plasmas," J. Phys. B: At. Mol. Opt. Phys. **44**, 180201 (2011).
5. H. Weimer, M. Müller, H. P. Büchler, and I. Lesanovsky, "Digital quantum simulation with rydberg atoms," Quantum Inf. Process. **10**, 885–906 (2011).
6. C. G. Wade, N. Šibalić, N. R. de Melo, J. M. Kondo, C. S. Adams, and K. J. Weatherill, "Real-time near-field terahertz imaging with atomic optical fluorescence," Nat. Photonics **11**, 40–43 (2017).
7. J. A. Sedlacek, A. Schwettmann, H. Kübler, R. Löw, T. Pfau, and J. P. Shaffer, "Microwave electrometry with rydberg atoms in a vapour cell using bright atomic resonances," Nat. Phys. **8**, 819–824 (2012).
8. M. Jing, Y. Hu, J. Ma, H. Zhang, L. Zhang, L. Xiao, and S. Jia, "Atomic superheterodyne receiver based on microwave-dressed rydberg spectroscopy," Nat. Phys. **16**, 911–915 (2020).
9. J. D. Carter, O. Cherry, and J. Martin, "Electric-field sensing near the surface microstructure of an atom chip using cold rydberg atoms," Phys. Rev. A **86**, 053401 (2012).
10. K.-Y. Liao, H.-T. Tu, S.-Z. Yang, C.-J. Chen, X.-H. Liu, J. Liang, X.-D. Zhang, H. Yan, and S.-L. Zhu, "Microwave electrometry via electromagnetically induced absorption in cold rydberg atoms," Phys. Rev. A **101**, 053432 (2020).
11. B. Kim, K.-T. Chen, C.-Y. Hsu, S.-S. Hsiao, Y.-C. Tseng, C.-Y. Lee, S.-L. Liang, Y.-H. Lai, J. Ruseckas, G. Juzeliūnas *et al.*, "Effect of laser-frequency fluctuation on the decay rate of rydberg coherence," Phys. Rev. A **100**, 013815 (2019).
12. S. Sevinçli, C. Ates, T. Pohl, H. Schempp, C. Hofmann, G. Günter, T. Amthor, M. Weidemüller, J. Pritchard, D. Maxwell *et al.*, "Quantum interference in interacting three-level rydberg gases: coherent population trapping and electromagnetically induced transparency," J. Phys. B: At. Mol. Opt. Phys. **44**, 184018 (2011).
13. U. Raitzsch, R. Heidemann, H. Weimer, B. Butscher, P. Kollmann, R. Löw, H. Büchler, and T. Pfau, "Investigation of dephasing rates in an interacting rydberg gas," New J. Phys. **11**, 055014 (2009).
14. D. Tong, S. Farooqi, E. Van Kempen, Z. Pavlovic, J. Stanojevic, R. Côté, E. Eyler, and P. Gould, "Observation of electric quadrupole transitions to rydberg n d states of ultracold rubidium atoms," Phys. Rev. A **79**, 052509 (2009).
15. L.-M. Wang, X.-M. Liu, H. Zhang, J.-L. Che, Y.-G. Yang, J.-M. Zhao, and S.-T. Jia, "Measurements of relative transition oscillator strengths of rydberg states in cesium magneto-optical trap," J. Phys. Soc. Jpn. **81**, 104302 (2012).
16. J. J. Kay, S. L. Coy, B. M. Wong, C. Jungen, and R. W. Field, "A quantum defect model for the s, p, d, and f rydberg series of caf," The J. Chem. Phys. **134**, 114313 (2011).
17. Z.-G. Feng, L.-J. Zhang, J.-M. Zhao, C.-Y. Li, and S.-T. Jia, "Lifetime measurement of ultracold caesium rydberg states," J. Phys. B: At. Mol. Opt. Phys. **42**, 145303 (2009).
18. Z. Feng, H. Zhang, J. Che, L. Zhang, C. Li, J. Zhao, and S. Jia, "Collisional loss of cesium rydberg atoms in a magneto-optical trap," Phys. Rev. A **83**, 042711 (2011).
19. Z.-G. Feng, L.-J. Zhang, H. Zhang, J.-M. Zhao, C.-Y. Li, and S.-T. Jia, "Collisional cross-sections measurement of ultracold caesium rydberg states," EPL (Europhysics Lett. **92**, 13002 (2010).
20. K. Weatherill, J. Pritchard, R. Abel, M. Bason, A. Mohapatra, and C. Adams, "Electromagnetically induced transparency of an interacting cold rydberg ensemble," J. Phys. B: At. Mol. Opt. Phys. **41**, 201002 (2008).
21. Y.-W. Guo, S.-L. Xu, J.-R. He, P. Deng, M. R. Belić, and Y. Zhao, "Transient optical response of cold rydberg atoms with electromagnetically induced transparency," Phys. Rev. A **101**, 023806 (2020).
22. S. Bao, H. Zhang, J. Zhou, L. Zhang, J. Zhao, L. Xiao, and S. Jia, "Polarization spectra of zeeman sublevels in rydberg electromagnetically induced transparency," Phys. Rev. A **94**, 043822 (2016).
23. S. Bao, H. Zhang, J. Zhou, L. Zhang, J. Zhao, L. Xiao, and S. Jia, "Tunable frequency stabilization to zeeman sublevel transitions between an intermediate state and rydberg states," Laser Phys. **27**, 015701 (2016).
24. J. Ma, J. Wu, Y. Zhao, L. Xiao, and S. Jia, "Determination of the rotational constant of the cs_2 $0_g^-(6s+6p_{3/2})$ state by trap loss spectroscopy," Opt. Express **18**, 17089–17095 (2010).
25. J. Wu, Z. Ji, Y. Zhang, L. Wang, Y. Zhao, J. Ma, L. Xiao, and S. Jia, "High sensitive determination of laser-induced frequency shifts of ultracold cesium molecules," Opt. Lett. **36**, 2038–2040 (2011).
26. D. Manzano, "A short introduction to the lindblad master equation," AIP Adv. **10**, 025106 (2020).
27. Z. Zhang, Y. Peng, C. Li, Z. Jia, D. Li, and Q. Zeng, "Proposal for measurement of the van der waals interaction in a cold rydberg ensemble via electromagnetically induced transparency," J. Opt. Soc. Am. B **36**, 2216–2220 (2019).
28. D. Yan, B. Wang, Z. Bai, and W. Li, "Electromagnetically induced transparency of interacting rydberg atoms with two-body dephasing," Opt. Express **28**, 9677–9689 (2020).
29. Z. Bai, C. S. Adams, G. Huang, and W. Li, "Self-induced transparency in warm and strongly interacting rydberg gases," Phys. Rev. Lett. **125**, 263605 (2020).